Biomaterials 30 (2009) 5523–5533

Contents lists available at ScienceDirect

Biomaterials

journal homepage: www.elsevier.com/locate/biomaterials

Intervertebral disc regeneration in an *ex vivo* culture system using mesenchymal stem cells and platelet-rich plasma

Wei-Hong Chen [a,b,1], Hen-Yu Liu [c,1], Wen-Cheng Lo [d,1], Shinn-Chih Wu [e], Chau-Hwa Chi [f], Hsueh-Yuan Chang [g], Shih-Hsiang Hsiao [e], Chih-Hsiung Wu [h], Wen-Ta Chiu [i], Bao-Ji Chen [e], Win-Ping Deng [a,b,j,*]

[a] *Stem Cell Research Center, Taipei Medical University, Taipei, Taiwan, ROC*
[b] *Graduate Institute of Biomedical Materials and Engineering, Taipei Medical University, Taipei, Taiwan, ROC*
[c] *Graduate Institute of Medical Sciences, Taipei Medical University, Taipei, Taiwan, ROC*
[d] *Department of Neurosurgery, Taipei Medical University, Taipei, Taiwan, ROC*
[e] *Department of Animal Science and Technology, National Taiwan University, Taipei, Taiwan, ROC*
[f] *School of Veterinary Medicine, National Taiwan University, Taipei, Taiwan, ROC*
[g] *School of Pharmacy, College of Medicine, National Taiwan University, Taiwan, ROC*
[h] *Division of General Surgery, Department of Surgery, Taipei Medical University, Taiwan, ROC*
[i] *Department of Neurosurgery, Taipei Medical University–Wan Fang Hospital, Taipei, Taiwan, ROC*
[j] *Cancer Center, Taipei Medical University Hospital, Taipei, Taiwan, ROC*

ARTICLE INFO

Article history:
Received 15 April 2009
Accepted 8 July 2009
Available online 30 July 2009

Keywords:
Intervertebral disc
Mesenchymal stem cell
Platelet-rich plasma
Nucleus pulposus
Regeneration

ABSTRACT

An *ex vivo* degenerative intervertebral disc (IVD) organ culture system was established for the screening of disc regeneration agents. Its application was demonstrated by a stem cell and growth factor-based therapeutic approach for the amelioration of IVD. An *ex vivo* culture system using chymopapain to partially digest nucleus proposus tissue was established to mimic human IVD degeneration. This system was then used for the evaluation of different therapeutic regimens including: mesenchymal stem cell derived from eGFP-transgenic porcine (MSC-GFP), platelet-rich plasma (PRP) and MSC-GFP/PRP combined treatment, and confirmed in *in vivo* animal model. Chondrogenic-specific gene products including *Col II* and *aggrecan* were found upregulated and chondrogenic matrix deposition increased, as evident by sustained fluorescent signals over 4 weeks, in the MSC-GFP implanted group. Previously, we demonstrated *in vitro* stage-specific chondrogenesis of MSC by chondrocytic commitment. These same molecules upregulated for chondrogenesis were also observed in MSC-GFP group. PRP that has been shown to promote nucleus pulposus (NP) regeneration also resulted in significant increased levels of mRNA involved in chondrogenesis and matrices accumulation. The *ex vivo* IVD regeneration results were repeated and supported by *in vivo* porcine degenerative system. Moreover, the disc height index (DHI) was significantly increased in both *in vivo* MSC-GFP and PRP regeneration groups. Unexpectedly, the MSC-GFP/PRP combined therapy demonstrated an inclination towards osteogenesis in *ex vivo* system. The *ex vivo* degenerative IVD culture system described in this study could serve as an alternative and more accessible model over large animal model. This system also provides a high-throughput platform for screening therapeutic agents for IVD regeneration.

1. Introduction

Low back pain (LBP) induced by intervertebral disc (IVD) degeneration has excruciated approximately 80% aging population and caused a significant socio-economic problem [1]. The tissue degeneration often originated from the high degradation of proteoglycan composites in nucleus pulposus (NP), and the extracellular matrix (ECM) was subsequently altered, representing the major pathogenic characterization of IVD degeneration [2]. In the multiple and complex process of IVD degeneration, the breakdown of cross-link in collagen fibers and disorganizations of proteoglycan composites will result in structural deformation and dehydration in discs, respectively [3]. Hence, therapeutic strategies for IVD degeneration have become emergent to be further developed. The

* Corresponding author. Institute of Biomedical Materials and Engineering, Taipei Medical University, 250 Wu-Hsing Street, Taipei 110, Taiwan, ROC. Tel.: +886 2 2739 0863; fax: +886 2 2739 5584.
E-mail address: wpdeng@ms41.hinet.net (W.-P. Deng).
[1] These authors contributed equally to this work.

0142-9612/$ – see front matter © 2009 Elsevier Ltd. All rights reserved.
doi:10.1016/j.biomaterials.2009.07.019

animal models have been applied for the transition from bench to bed-side and provide information of cell biology and biochemistry of IVD tissue closely resembling those in human beings [4,5]. Larger animal models, including primates, porcine, sheep, etc., have been widely used for disc physiological studies [6–9]. Among these animal models, porcine possess more similarities to human in tissue composition and sizes of lumbar segments [10].

The IVD is a highly differentiated tissue with the avascular nature. The anabolic and metabolic molecules for disc cellular physiology are extracellularly supplied by diffusion from the neighbor tissue such an annulus fibrous (AF) and endplate [11]. Daniel et al. established a disc/endplate whole IVD organ culture system with preserved cell functions [12]. Gene-delivered cell therapy has also been examined in rabbit IVD organ culture system [13]. However, healthy cultured IVD tissue without injuries cannot actually represent clinical pathological and degenerative disc. To develop a diseased IVD with degraded disc matrix and degenerative NP cell is urgent. Chymopapain has been reported as an alternative clinical treatment modality for lumbar disc herniation [14]. With its chemonucleolysis by degrading the proteoglycan structure and destructing the matrix in NP tissue, the chymopapain might be an agent candidate to establish degenerative model.

Many injection strategies of cells and growth factor therapies for intervertebral disc (IVD) regeneration have been developed [5,15–17]. Cell therapy with mesenchymal stem cells (MSC) has become an attractive method for treating IVD degeneration [16,18]. Zhang et al. showed that MSC transplantation in rabbit IVD can induce proteoglycan synthesis [19]. MSC differentiating into NP-like cells was reported by coculturing with mature NP cells [20]. The MSC in chondrogenic tissue engineering and its stage-specific molecular pathways by which MSC could be committed into chondroprogenitors were also addressed in our previous studies [21,22]. Since IVD tissue was suggested as an immune-privileged circumstance due to its avascular characteristic, MSC that can escape alloantigen recognition could be a cell therapy candidate in clinical IVD regenerative therapies [23]. Moreover, differentiation behaviors of MSC implanted in the degenerative disc organ are needed to be further investigated.

Growth factors derived from mammalian tissues have been defined as protein molecules to regulate cell proliferation, tissue growth and organism development [24]. The *in vivo* and *in vitro* effects of growth factors on IVD tissue are by regulating the cell proliferation and chondrogenic matrix metabolism [17,25,26]. Platelet-rich plasma (PRP) purified from whole blood comprised many growth factors, such as transforming growth factor β1 (TGF-β1), platelet-derived growth factors (PDGF), insulin-like growth factor (IGF), etc. and was defined as a growth factor cocktail [27,28]. We have previously examined the potential of PRP on human NP cells, including promoting cell proliferation, redifferentiation and reconstitution of human NP tissue [29]. We also demonstrated the role of TGF-β1 in PRP leading to IVD regeneration. Hence, PRP will be a good therapeutic candidate for IVD regeneration in this study.

Previously, we demonstrated the *in vitro* stage-specific chondrogenesis of stem cell committed by chondrocytic circumstance [21]. In this study, our goal is to create a novel *ex vivo* degenerative whole-organ IVD culture system to regenerate nucleus pulposus (NP) tissue, which provides a closed and feasible chondrocytic environment. The MSC or PRP was used as a therapeutic agent candidate. Porcine was selected as an animal model to perform the therapeutic system to mimic human species due to their similar anatomy and physiology [30]. The chondrogenic regenerative potentials of stem cells and PRP that have been examined in our previous studies [21,29] were used in the *ex vivo* system to demonstrate its applications. To confirm the efficacies of *ex vivo* culture system, two approaches including MSC-GFP only and PRP only (derived from our *ex vivo* results) were selected to perform in the *in vivo* animal system.

2. Materials and methods

2.1. Establishment of ex vivo organ cultures of degenerative IVD tissue

Miniature porcine ($N = 5$, 2–3 month, 15–20 kg) were sacrificed and the complete IVD tissue [including partial vertebrate body (VB), endplates (EP), nucleus pulposus (NP) and annulus fibrous (AF)] of lumbar spine from T13 to L5 (6 IVDs/porcine) were harvested under aseptic conditions (Fig. 1A). Chymopapain (Sigma, St. Louis, MO) was then injected into the central region of disc with 20 G spinal needle (MEDITOP Corporation, Malaysia) to create disc degeneration model. Subsequently, IVD tissue was cultured in DMEM with 10% FBS incubated in a humidified 5% CO_2 atmosphere at 37 °C as previously described [12,31]. After 1 week cultivation, digested tissues were washed with PBS and designed therapeutic substrates such as MSC-GFP, PRP, the combined therapy of MSC-GFP/PRP and saline were injected into the defected site. The *ex vivo* IVD organ cultures were maintained in DMEM + 10% FBS and then harvested after 4 weeks for chondrogenic characteristics by following analysis.

2.2. Creation of in vivo IVD degeneration in porcine model

Meanwhile, the *in vivo* porcine model was also established to confirm the feasibilities of *ex vivo* culture system (Fig. 1B). The animal experiment protocol was approved by the Institutional Animal Care and Use Committee of Taipei Medical University. Miniature porcine were anesthetized and their locations of T13-L5 IVDs were oriented based on X-ray. 200 U chymopapain (Sigma) was then injected into the central NP tissue with 20 G spinal needle (MEDITOP Corporation, Malaysia) for 1 week to create *in vivo* disc degeneration in porcine model. Experimental groups ($N = 3$ in each group) were designed as: (a) normal control (NC); (b) MSC-GFP injection; (c) PRP injection; chymopapain injected as negative control group. Porcine were then fed under healthy conditions for 2 months and sacrificed to harvested discs for genetic and histological analysis.

2.3. Purification of MSC from eGFP-transgenic porcine

MSC were isolated from bone marrow of eGFP-transgenic porcine by gradient isolation of mononuclear cells under sterile conditions and designated as MSC-GFP. Briefly, 40 ml of bone marrow were collected by aspiration from the iliac crest of eGFP-transgenic porcine and centrifuged using 600*g* for 30 min. Mononucleated cells were recovered from the middle layer, washed three times with phosphate-buffered saline (PBS) and finally seeded on culture plates with MEM + 10% FBS culture medium. Cells that adhered to culture plates will then form colonies and expanded in monolayer culture for subsequent assay.

2.4. Multilineage differentiation abilities of MSC-GFP

For determining the multilineage differentiation of MSC-GFP, cells were treated with the following culture conditions: (a) Osteogenesis: MEM supplemented with 10% FBS, 50 μg/ml ascorbate-2 phosphate (Sigma), 10^{-8} M dexamethasone (Sigma) and 10 mM β-glycerophosphate (Sigma); (b) Adipogenesis: MEM supplemented with 10% FBS, 50 μg/ml ascorbate-2 phosphate, 10^{-7} M dexamethasone, 50 μg/ml indomethacin (Sigma), 0.45 mM 3-isobutyl-1-methylxanthine (Sigma) and 10 ng/ml insulin (Sigma); (c) Chondrogenesis: cell pellets formed by MSC-GFP cultured in MEM supplemented with ITS$^+$ Premix (GIBCO) and 10 ng/ml TGF-β1 (Preprotech, Rocky Hill, NJ); (iv) Neurongenesis: cells were cultured in MEM supplemented with 10% FBS, 10% FCS and 1 mM β-mercaptoethanol (Sigma) for 24 h, the serum then being removed and the culture continued for 5 h to 5 days. After the appearance of morphologic features of MSC-GFP through differentiation process, cells were assayed by specific matrix stainings and phenotypic detections.

2.5. PRP preparation and TGF-β1 concentration evaluation

Total blood was purified from porcine and driven into MCS blood cell separation system (Haemonetics Corporation, USA). As the same process shown in our previous study [29], bovine thrombin (100 IU bovine thrombin/150 ml PRP) was then added to the solution, shakes to remove the aggregated fibrin, and centrifuged for 6 min, 3000 rpm at room temperature. To confirm the consistency of PRP for *ex vivo* and *in vivo* utilization and to determine the most appropriate concentration for study, TGF-β1 was quantitatively analyzed using a Quantikine enzyme-linked immunosorbent assay (ELISA) kit (#DB100, R&D Diagnostics, Wiesbaden, Germany), and used as the core ingredient of PRP. A dilution series of TGF-β1 standards (#890207) was prepared in 100-μl volumes in 96-well microtiter plates coated with TGF-β1-receptor II. The 0.1 ml PRP solution was then mixed with 0.1 ml 2.5 N acetic acid/10 M urea, incubated at room temperature for 10 min, and neutralized by an addition of 0.1 ml of 2.7 N NaOH/1 M HEPES (*N*-[2-hydroxyethyl] piperazine-*N*′-[2-ethanesulfonic acid]; Sigma) (#H-7523).

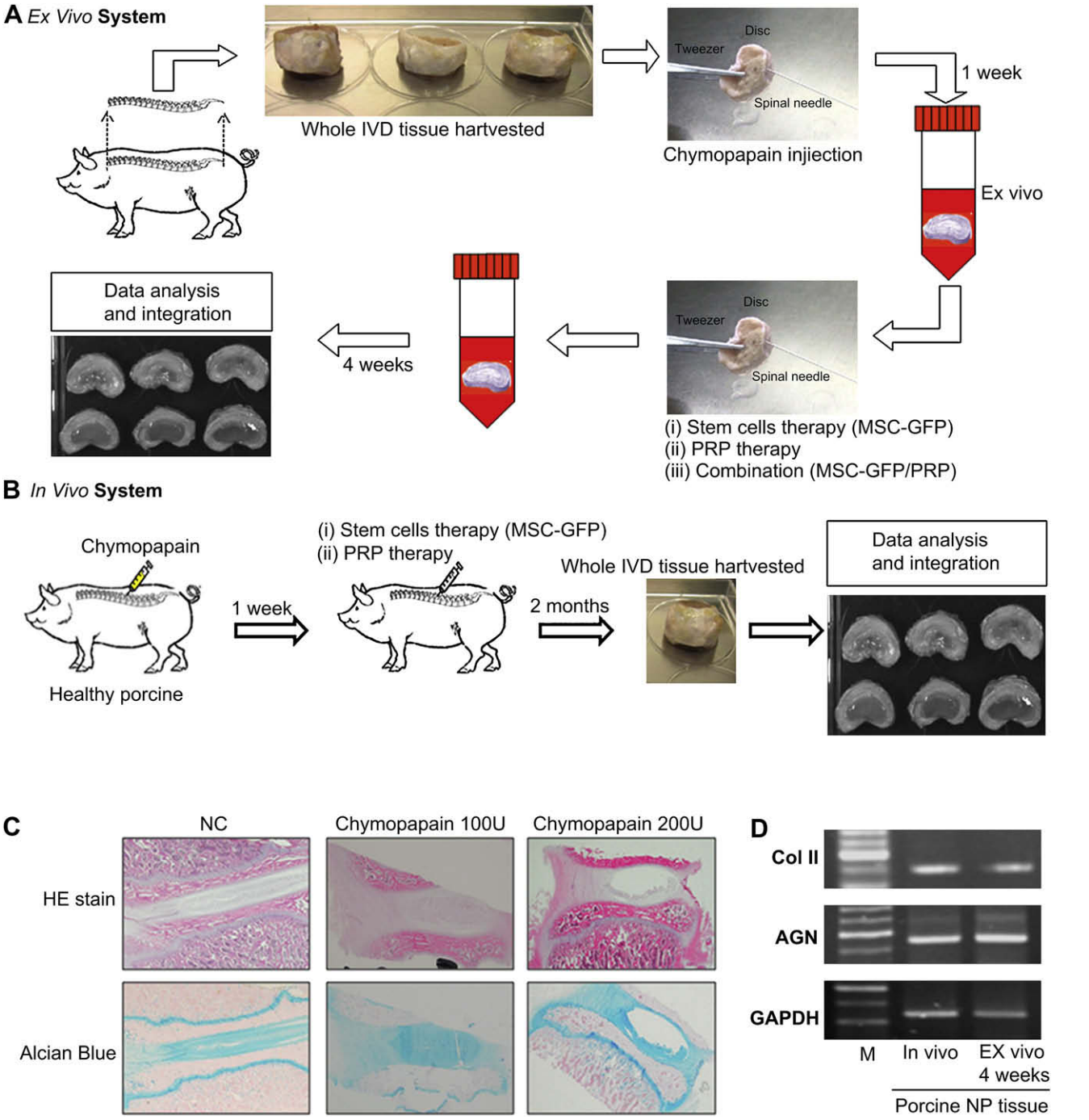

Fig. 1. Establishment of *ex vivo* and *in vivo* intervertebrate disc (IVD) degeneration systems. (A) Schematic description of degenerated *ex vivo* whole IVD tissue culture system which was then treated by stem cells or/and PRP. (B) *In vivo* IVD degeneration system was created directly on porcine model to confirm the applicability of *ex vivo* IVD culture system. (C) Histological determinations of degenerative IVD tissue by chymopapain injection. Matrix degradation of nucleus pulposus (NP) tissue was evaluated by HE stain and Alcian blue stain. (D) Transcriptional comparisons of chondrogenic-specific genes including type II collagen (Col II) and aggrecan (AGN) between *in vivo* and *ex vivo* 4-week cultured IVD tissue.

2.6. Semi-quantitative reverse transcription polymerase chain reaction

Total RNA from cells were extracted using TRIzol® reagent (Invitrogen Life Technologies, Carlsbad, CA, USA) and subjected to reverse transcription by SuperScript™ III (Invitrogen Life Technologies) to produce cDNA. Six microliters of cDNA was used for amplification reaction in a final volume of 50 μl containing 2.5 mM dNTP, 25 mM $MgCl_2$, primers (listed in Table 1) and *Taq* DNA polymerase (Invitrogen). Gene amplification reaction was carried out using Touchgene Gradient PCR machine (Techne, Cambridge, UK) and the annealing temperatures (between 55 and 65 °C) used differed depending on the genes of interest. Finally, PCR products were then run on agarose gels (Agarose I; AMRESCO, OH, USA) and visualized with ethidium bromide (EtBr) staining. Images were analyzed using FloGel-I (Fluorescent Gel Image System; TOP BIO Co., Taiwan). Glyceraldehyde 3-phosphate dehydrogenase (GAPDH) was used as an internal control.

2.7. Macroscopic and fluorescent observations

After 2-month *ex vivo* cultures, IVDs were horizontally dissected and observed by high resolution CCD (UVP, BioSpectrum® Imaging System) for their tissue completeness, water maintenance, and macromorphologies. For detecting MSC-GFP proliferation in IVD, their GFP expression signal was determined using Imaging System 200 Series (Xenogen Corporation, Alameda, CA) under a 488 nm excitation light.

Table 1
Primer sequences for PCR products to determine multilineage potentials of MSC-GFP.

Specific genes	Primer sequences (5′ to 3′)
GAPDH	P1: GCT CTC CAG AAC ATC ATC CCT GCC
	P2: CGT TGT CAT ACC AGG AAA TGA GCT T
Type II collagen (Col II)	P1: TTC TGA GAG GTC TTC CTG GC
	P2: AAT ACC AGC AGC TCC CCT CT
Aggrecan	P1: CAG GTG AAG ACT TTG TGG ACA TC
	P2: GTG AGT AGC GGG AGC CC
Osteocalcin	P1: CAG ATC CTC TGG AGC CCA GG
	P2: CTT ACA CTT GCC GGG CAG GG
Osteopontin	P1: ACG ACG CTG ACC GAT CC
	P2: TGT CTT CTT CGC TCT TAG AGT C
PPARγ2	P1: CGC CCC TGG CAA AGC ACT
	P2: TCC ACG GAG CGA AAC TGA CAC
AP2	P1: GGC CAA ACC CAA CCT GA
	P2: GGG CGC CTC CAT CTA AG
GFAP	P1: ACA TCG AGA TCG CCA CCT AC
	P2: ACA TCA CAT CCT TGT GCT CC

2.8. Real-time polymerase chain reaction

cDNA were prepared from extracted RNA of NP tissue from *ex vivo* and *in vivo* IVDs as previously described. Products were then performed on LightCycler Instrument (LC 2.0, Roche, Germany) using the FastStart DNA Master SYBR Green I Kit (Roche Diagnostics) to detect following genes: type II collagen: 5′-CCA TCT GGC TTC CAG GGA C-3′, 5′-CCA CGA GCC AGG GCT-3′; aggrecan: 5′-TGC AGG TGA CCA TGG CC-3′, 5′-CGG TAA TGG AAC ACA ACC CCT-3′. Fluorescence was measured using channel F1 after elongation at each cycle and T_m values were manually assigned from a plot generated by the Roche LightCycler instrument of the negative derivation of fluorescence versus temperature ($-dF/dT$) of the melting curve for amplification products measured at 530 nm. For each sample the threshold cycle (C_T) values were determined automatically by the LightCycler software (Roche) and relative changes among experimental and control groups in gene expression were determined by the $2^{-\Delta\Delta C_T}$ method.

2.9. Detections of chondrogenic and osteogenic matrix accumulations

IVD specimens from *ex vivo* and *in vivo* system were harvested and fixed in 4% phosphate-buffered formaldehyde, embedded within paraffin and sectioned (7–10 μm). For chondrogenic ECM detections, type II collagen monoclonal antibody (Chemicon International, Temecula, CA, USA) was used in immunohistochemistry (IHC) which only reacts with type II collagen while Alcian blue staining was utilized for detecting synthesized proteoglycan arranged in IVD tissue. For the osteogenic matrix accumulations, alkaline phosphatase (ALPase) activity was measured using a biochemical assay (Sigma), based on conversion of *p*-nitrophenyl phosphate to *p*-nitrophenol. Furthermore, the von Kossa staining was used to identify the mature bone matrix mineralization.

2.10. Creation of in vivo IVD degeneration in porcine model

The animal experiment protocol was approved by the Institutional Animal Care and Use Committee of Taipei Medical University. As shown in Fig. 1B, miniature porcine were anesthetized and their locations of T13-L5 IVDs were oriented based on X-ray. 200 U chymopapain (Sigma) was then injected into the central NP tissue with 20 G spinal needle (MEDITOP Corporation, Malaysia) for 1 week to create *in vivo* disc degeneration in porcine model. Experimental groups ($N = 3$ in each group) were designed as: (a) normal control (NC); (b) MSC-GFP injection; (c) PRP injection;

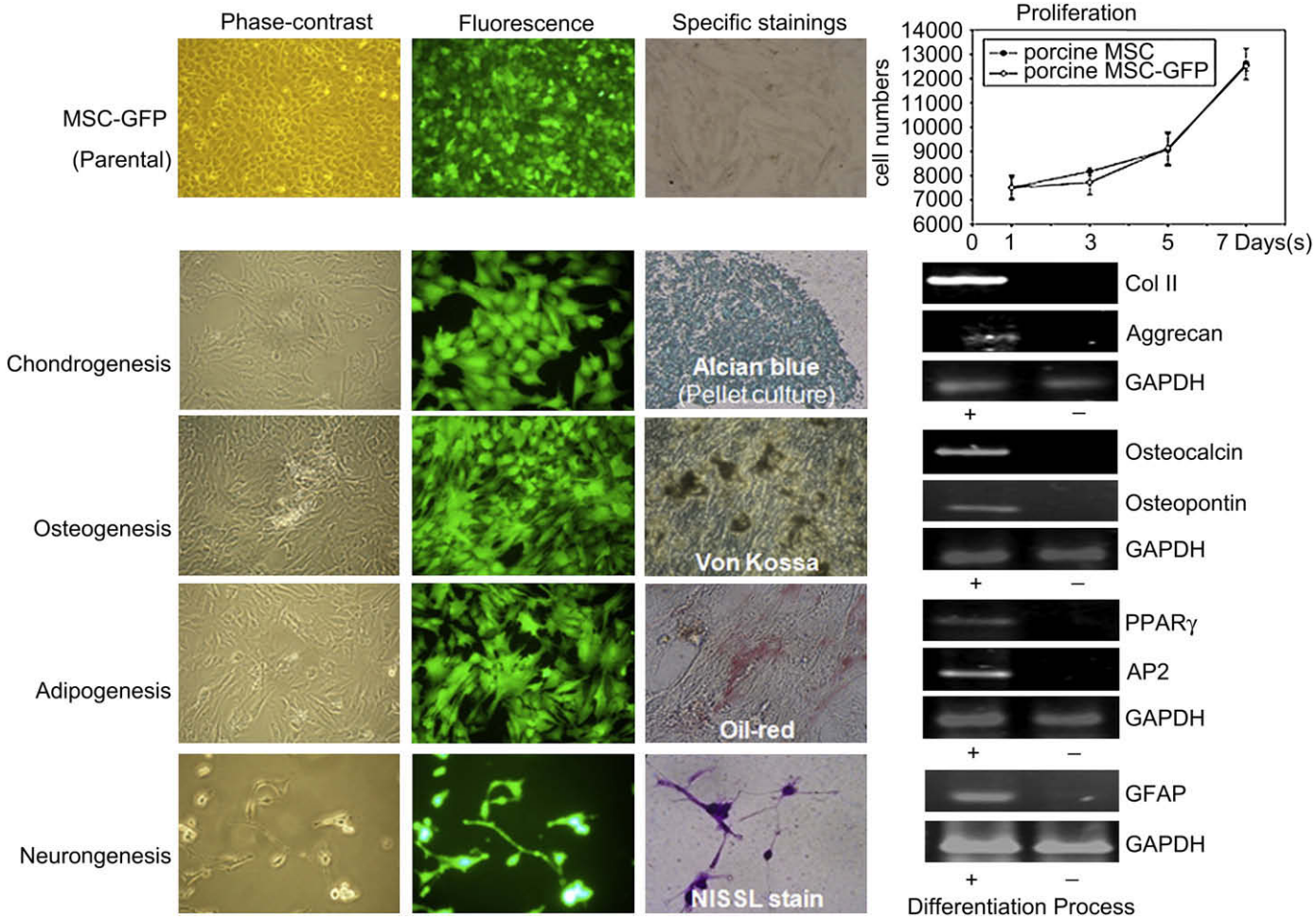

Fig. 2. Multilineage potentials of MSC-GFP under specific induction culture conditions. Cell appearances were shown using phase-contrast and fluorescent microscope for their morphological changes (left two panels). Cell proliferation showed no difference between MSC with (porcine MSC-GFP) and without GFP (porcine MSC) (left upper panel). Specific marker stainings and RT-PCR were used to determine MSC-GFP undergoing chondrogenesis, osteogenesis, adipogenesis and neurongenesis (right two panels).

chymopapain injected as negative control group. Porcine were then fed under healthy conditions for 2 months and sacrificed to harvested discs for genetic and histological analysis.

2.11. Disc height index

Disc height of porcine from treatment and control groups was analyzed using X-ray radiographs. Images including disc height and vertebral body height were measured and their disc height index (DHI) was calculated by the following function: DHI = BC + EF/AB + DE (as shown in Fig. 5A). Changes of DHI among experimental porcine after operation were expressed as DHI percentage and subsequently normalized to their preoperative DHI [% DHI = (postoperative DHI/preoperative DHI) × 100%]. Values were plotted by using SigmaPlot.

2.12. Statistical analysis

The data on *in vivo* and *ex vivo* gene expressions and DHI were analyzed using paired *t*-test to evaluate the efficiencies of each experiment groups compared to the

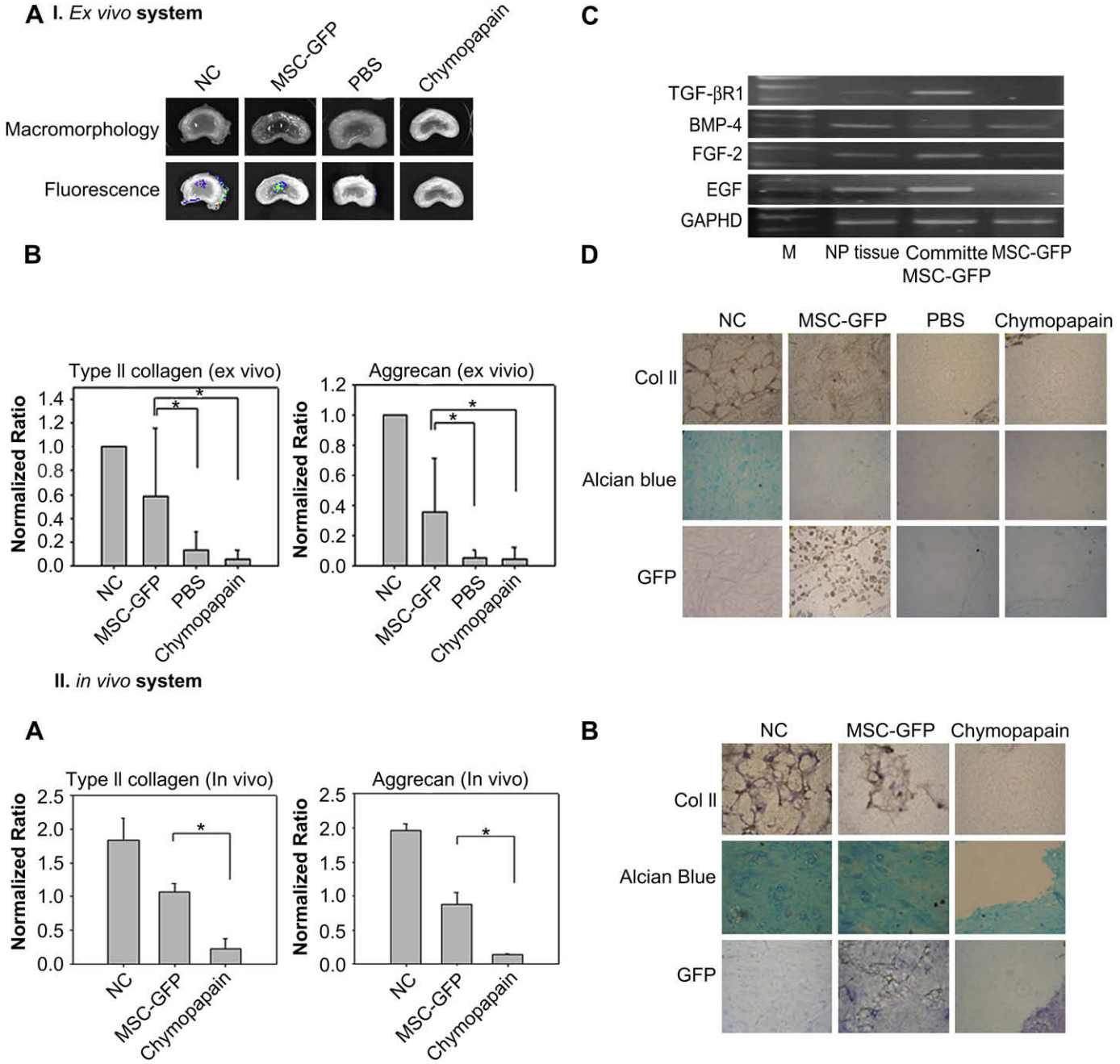

Fig. 3. Evaluations of regeneration efficacy of MSC-GFP in *ex vivo* and *in vivo* degenerative IVD system. (I) *Ex vivo* system: (A) Morphologic appearance of IVD tissue among normal control (NC), MSC-GFP, PBS and chymopapain groups. Macromorphologies and fluorescent signals were detected by using UVP and IVIS 200, respectively. (B) Chondrogenic-specific mRNA such as Col II and AGN were analyzed using real-time PCR and respective expressions were normalized to individual glyceraldehyde phosphate dehydrogenase (GAPDH). Results are shown as the mean ± S.D. for 3 independent experimental cultures. $^{*}p < 0.05$, compared with chymopapain treated only group using paired *t*-test. (C) NP developmental molecules were activated in committed MSC-GFP in *ex vivo* IVD tissue cultures. GAPDH was used as internal control. (D) Histological analysis of NP tissue among experimental and control groups. Row 1 and row 2, chondrogenic extracellular matrix (ECM) accumulations were detected through immunohistochemistry (IHC) for Col II and Alcian blue specific staining for proteoglycan. Row 3, IHC of green fluorescence protein (GFP). All panels are representative of 3 separate experiments (400×). (II) *In vivo* animal model: (A) Real-time PCR represents chondrogenic-specific mRNA and normalized to individual GAPDH. Results are shown as the mean ± S.D. for 3 independent experimental cultures. $^{*}p < 0.05$, compared with chymopapain treated only group using paired *t*-test. (B) Histological analysis of NP tissue from NC, MSC-GFP and chymopapain groups by IHC and specific stainings (400×). IHC of GFP was used to detect the growth of MSC-GFP in NP tissue.

chymopapain group. Data were shown as mean ± standard deviation (SD) and considered statistically significant if p values were 0.05 or less.

3. Results

3.1. Experimental design

As shown in Fig. 1A for *ex vivo* system, miniature porcine were sacrificed and the whole IVD tissue of lumbar spine from T13 to L5 (6 IVDs/porcine) were harvested under aseptic conditions. To create NP tissue degeneration model in *ex vivo* platform, chymopapain was injected into disc for partial digestion. One week later, three therapeutic approaches including mesenchymal stem cells (MSC) only, PRP only, and the combined treatments were performed to restore the disc degeneration. After 4 weeks *ex vivo* tissue culture, regeneration efficiencies were analyzed by chondrogenic characteristics. Meanwhile, the *in vivo* system of porcine model (Fig. 1B) was also established to confirm the feasibilities of *ex vivo* culture system. After direct injection of chymopapain into lumbar spine of porcine body for one week, two approaches including MSC-GFP only and PRP only (derived from our *ex vivo* results) were selected to perform *in vivo* animal system. For two-month *in vivo* disc restoration, porcine were then sacrificed to harvest the whole IVD tissue for their chondrogenic characterizations.

The degeneration level of NP tissue created by chymopapain partial digestion was quantified by histological examination to determine the optimal dosage (Fig. 1C). Chymopapain of 200 U was selected as injection dose to keep the residual NP cells as template for tissue regeneration. Furthermore, we have also demonstrated that NP phenotypic markers gene expression in *ex vivo* system for 4-week culture was almost identical to these in *in vivo* system, according to the major chondrogenic genes type II collagen (Col II)

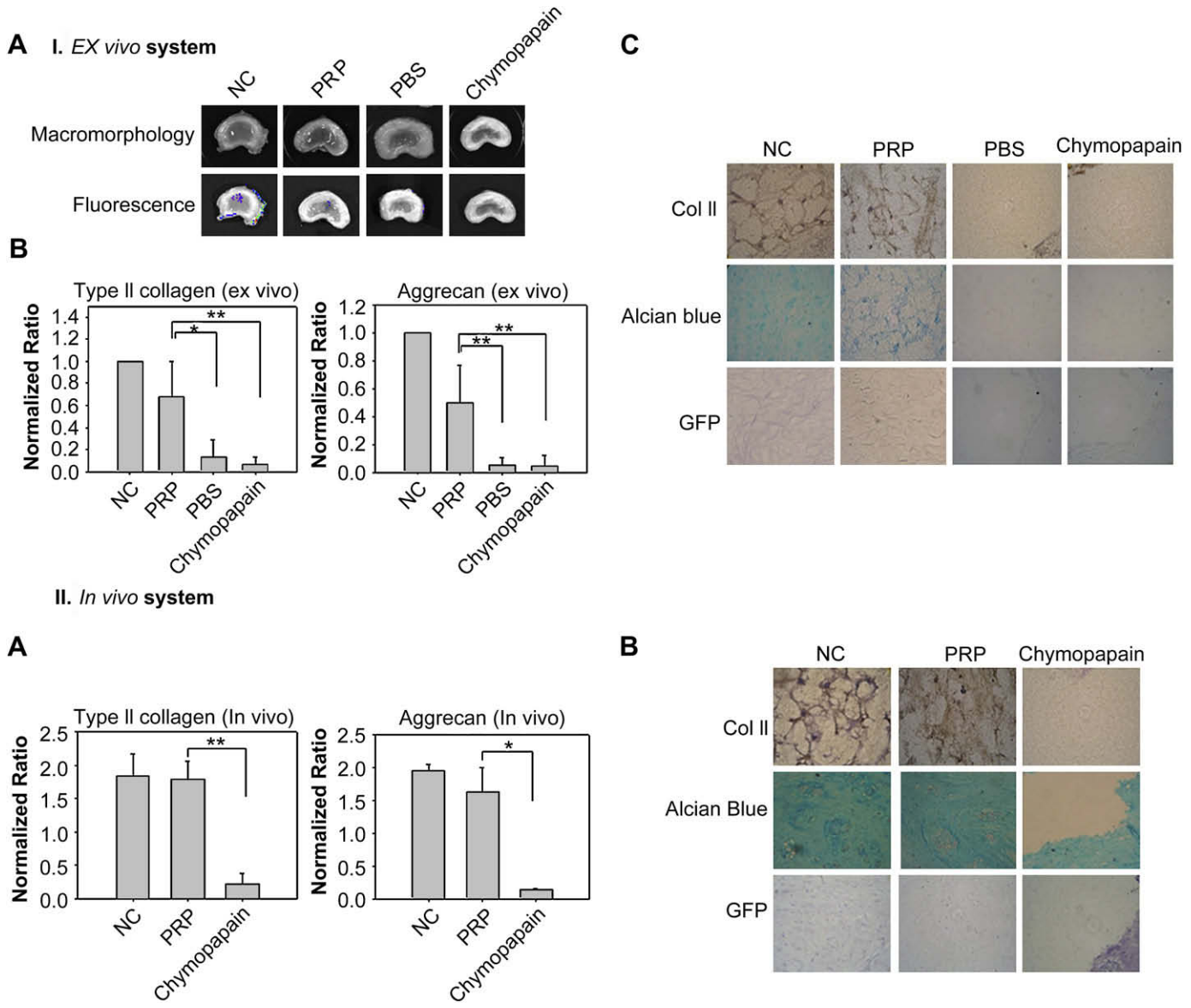

Fig. 4. Evaluations of regeneration efficacy of PRP in *ex vivo* and *in vivo* degenerative IVD system. (I) *Ex vivo* system: (A) Morphologic appearance of IVD tissue among NC, PRP, PBS and chymopapain groups. (B) Chondrogenic-specific mRNA were analyzed using real-time PCR and respective expressions were normalized to individual GAPDH. Results are shown as the mean ± S.D. for 3 independent experimental cultures. $^{*}p < 0.05$, $^{**}p < 0.01$, compared with chymopapain treated only group using paired t-test. (C) Histological analysis of NP tissue among experimental and control groups. (II) *In vivo* system: (A) Real-time PCR represents chondrogenic-specific mRNA and normalized to individual GAPDH. Results are shown as the mean ± S.D. for 3 independent experimental cultures. $^{*}p < 0.05$, $^{**}p < 0.01$ compared with chymopapain treated only group using paired t-test. (B) Histological analysis of NP tissue from NC, PRP and chymopapain groups by IHC staining (400×). The details are described in Fig. 3.

and aggrecan (AGN) (Fig. 1D). The results indicated that the *ex vivo* system might be considered as an alternative and easier approach for laborious *in vivo* system.

3.2. Multilineage potentials of MSC-GFP

MSC-GFP showed a fibroblast-like morphology and an endogenous fluorescence image (Fig. 2). To determine the differentiation potentials, MSC-GFP were cultured under standard induction procedures and distinct mesenchymal lineages including chondrogenesis, osteogenesis, adipogenesis and neurongenesis were shown for their specific phenotypes by using RT-PCR and marker stainings. In addition, proliferation assays showed no difference between MSC-GFP and MSC (purified from porcine, without eGFP transduced).

3.3. Macromorphology of IVD tissue MSC-GFP implantation

MSC-GFP was implanted into the central region of IVD after 1-week chymopapain treatment and whole organ were then cultured in DMEM/F12 with 10% FBS. During 4 weeks *ex vivo* culture, whole IVD tissues were harvested and cross sectioned to expose the NP and annulus fibrosus (AF) organization (Fig. 3, I-A). Macromorphologies of NP tissue from both normal control (NC) and MSC-GFP treatment group (MSC-GFP) showed more water-preserved and more tissue-saturated appearance under UVP detection, compared to the fibrosis appearance from PBS and chymopapain group. Intensive fluorescence signals from MSC-GFP group in the implanted region indicated the proliferation of implanted cells.

3.4. Ex vivo NP regeneration by MSC-GFP

For chondrogenic-specific mRNA detections, MSC-GFP also showed a significant restoration of type II collagen and aggrecan compared to the PBS and chymopapain control (Fig. 3, I-B, $N = 6$). To analyze the chondrogenesis process in committed MSC-GFP in *ex vivo* system, these IVD developmental molecules were examined in MSC-GFP implanted cultures (Fig. 3, I-C). The expressions of the FGF-2, EGF, and especially the TGF-βR1 were all strongly upregulated in 4-week *ex vivo* committed MSC-GFP compared to parental MSC-GFP. Interestingly, bone morphogenetic protein-4 (BMP-4) showed a moderate decrease.

To further determine the fate of implanted MSC-GFP in NP tissue, chondrogenic and osteogenic matrix accumulations were further detected in harvested NP tissue among designated groups after 4-week *ex vivo* tissue culture (Fig. 3, I-D). Immunohistochemistry (IHC) of type II collagen (Col II) and Alcian blue staining of proteoglycan showed an intensive and extensive signal in MSC-GFP implanted NP tissue, similar to the normal control (NC) group, but both not in PBS and chymopapain groups. Additionally, there was no apparent signal in the alkaline phosphatase (ALP) and von Kossa staining from either NC or MSC-GFP groups, indicating no osteogenesis in the regenerative tissue (data not shown). Moreover, PBS treatment or chymopapain only groups showed severe tissue loss so that no staining signal was detected. To assess the distribution of implanted MSC-GFP, the cells were stained positively with GFP antibody (Fig. 3I-D, bottom).

3.5. In vivo NP regeneration by MSC-GFP

To validate the results from *ex vivo* IVD culture system, the same therapeutic approaches were then repeated in *in vivo* porcine model. In Fig. 3II-A, significant upregulation of Col II and aggrecan in MSC-GFP group was detected compared to chymopapain group. Additionally, chondrogenic-specific matrices stainings, including IHC of Col II and Alcian blue of proteoglycan, presented highly extensive and intensive signals in the section of MSC-GFP implanted group and NC group (Fig. 3, II-B), and also no osteogenesis was observed through ALP and von Kossa staining (data not shown), supported by the *ex vivo* results. The distributions of MSC-GFP in chondrogenic ECM were also significantly detected by IHC of GFP (Fig. 3II-B, the lower panel).

3.6. Ex vivo/in vivo NP regeneration by PRP

In addition to the stem cell therapy group which showed strong potential in NP tissue regeneration, the second approach used to restore the residual NP cells was PRP. In our supplementary results, PRP promotes porcine NP (pNP) cell viability dose- and time-dependently *in vitro* (Supplemental Fig. 1A). Chondrogenic redifferentiation but not osteogenic differentiation of porcine NP was highly induced by PRP during 7-day treatment (Supplemental Fig. 1C). While introduced into *ex vivo* degenerative IVD model,

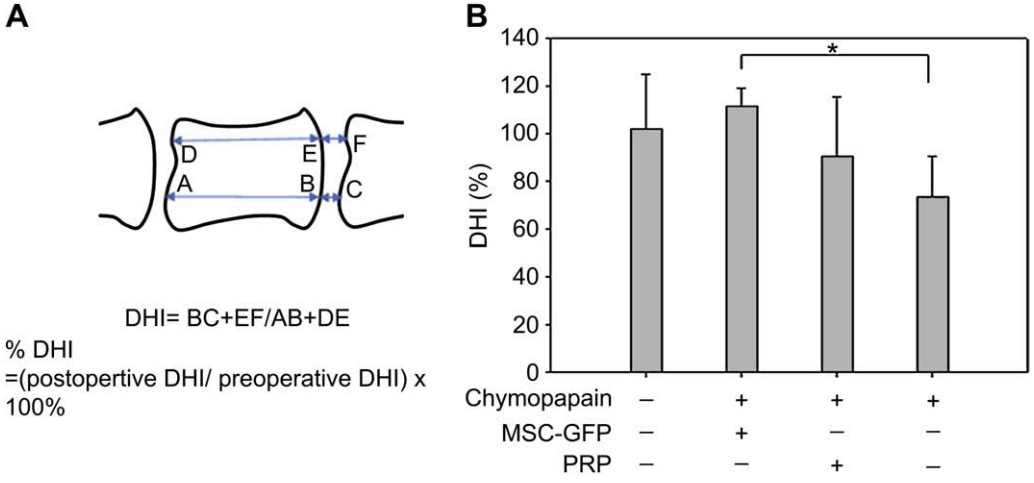

Fig. 5. Evaluation of *in vivo* disc height index (DHI). (A) DHI of IVD was measured by using indicated functions based on radiographic images. (B) Changes in the DHI after MSC-GFP or PRP injections for two months. The percentage of DHI from MSC-GFP, PRP and chymopapain groups was measured and normalized to the normal control. Results are shown as the mean ± S.D. for 6 independent discs. $^{*}p < 0.05$ compared with the chymopapain treated only group using paired *t*-test.

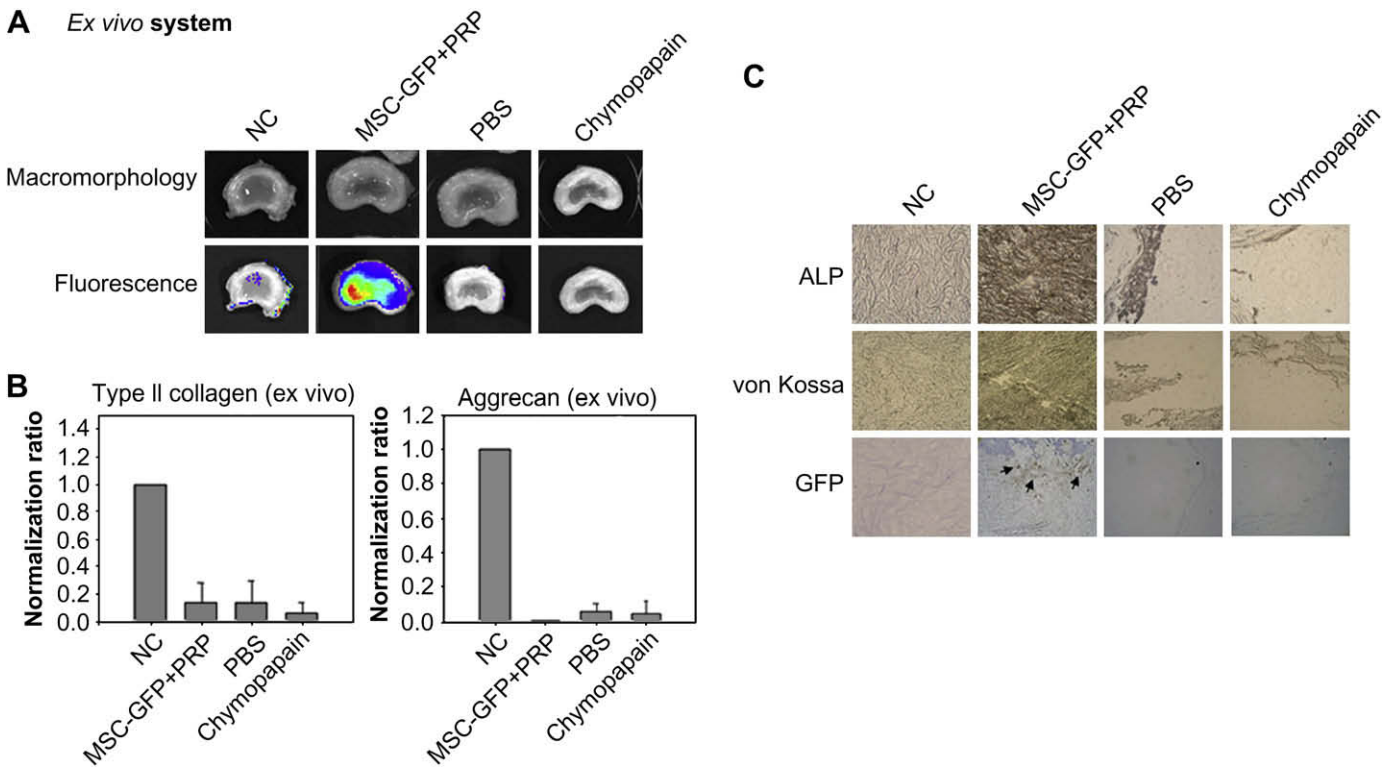

Fig. 6. Evaluations of regeneration efficacy of the combination of MSC-GFP and PRP in *ex vivo* degenerative IVD tissue culture system. (A) Morphologic appearance of IVD tissue among NC, MSC-GFP + PRP, PBS and chymopapain groups. (B) Chondrogenic-specific mRNA were analyzed using real-time PCR and respective expressions were normalized to individual GAPDH. Results are shown as the mean ± S.D. for 3 independent experimental cultures. $^{*}p < 0.05$, $^{**}p < 0.01$, compared with chymopapain treated only group using paired *t*-test. (C) Histological analysis of NP tissue among experimental and control groups. All panels are representative of 3 separate experiments (400×). The details are described in Fig. 3.

PRP-induced NP tissue formation with highly water content macromorphology similar to the normal control (Fig. 4, I-A). The elevated chondrogenic-specific mRNA was also detected through real-time PCR from regenerated tissue (Fig. 4, I-B). For the matrix accumulations (Fig. 4, I-C), strongly intensive and extensive signals were detected in both IHC of Col II and Alcian blue of proteoglycan in PRP group and NC group.

The same process was then examined using *in vivo* model. In Fig. 4IIA, the results showed that the mRNA level of type II collagen and aggrecan appeared almost identical in both PRP-induced and normal control groups, but not in chymopapain group. Histological analysis also represented intensive chondrogenic matrices accumulated in PRP group, resembling the normal control group (Fig. 4, II-B).

Otherwise, no osteogenic staining signals from ALP and von Kossa stainings were detected in normal control and PRP groups in both *ex vivo* and *in vivo* system (data not shown).

3.7. Disc height index

The disc height index (DHI, %) was evaluated based on radiographic images by the function in Fig. 5A. Based on normal control groups as standard level, the IVD space in chymopapain group shrank to 73 ± 16.96% ($N = 6$) after 2 months (Fig. 5B). However, the implantation of MSC-GFP showed a significant increase in disc height (111.6 ± 7.22%, $p < 0.05$, $N = 6$), and the injection of PRP also showed the recovery of disc height (91 ± 12.58%, $p = 0.5$, $N = 6$).

3.8. Determination of MSC-GFP/PRP combined treatment

Either MSC-GFP or PRP would induce chondrogenesis in both *ex vivo* and *in vivo* disc degeneration model. To determine if the combined treatment of MSC-GFP/PRP could restore the disc degeneration in an additive or synergistic manner, the effect of PRP on stem cells was examined by cell proliferation and gene expression. The results showed that PRP-induced MSC-GFP proliferation in a dose- and time-dependent manner during 7-day treatment (Supplemental Fig. 1B) and strongly upregulated osteogenic mRNA expressions such as osteocalcin and osteopontin (Supplemental Fig. 1D). The mixture of MSC-GFP and PRP was then applied on the *ex vivo* degenerated IVD model for 4 weeks (as shown in Fig. 1A). By macromorphological and fluorescence observations (Fig. 6A), the combined treatment group showed highly intensive fluorescent signals and fibrosis appearance through the central implanted region (NP) to the border region (AF). Neither type II collagen nor aggrecan was detected in MSC-GFP/PRP combination group by real-time PCR (Fig. 6B). Chondrogenic matrices were not formed by Col II of IHC and proteoglycan of Alcian blue staining examinations (data not shown). However, the osteogenic matrix accumulations examined by ALP and von Kossa stainings were both strongly induced (Fig. 6C). IHC of GFP that represented the proliferation of implanted MSC-GFP was also obviously upregulated, supported by the results from fluorescent images.

4. Discussion

Degeneration disc disease (DDD) has become an emergent problem affecting aging population, nevertheless, the optimal platform to evaluate the efficacies of degeneration treatment remains developed. In this study, we have established an *ex vivo* degenerative intervertebral disc (IVD) culture system for therapeutic agent screening, such as stem cell therapy and platelet-rich

plasma (PRP) therapy (Fig. 1A). The *ex vivo* culture system could preserve the complete *in vivo* IVD environment, because nutrients for *in vivo* IVD is permeated from surrounding vertebrates to endplate but not directly from blood vessels. It also provides closed native tissue architecture for disc cell proliferation within their specialized matrix [32,33] and a natural three dimensional structure for tissue engineering [34]. In Fig. 1D, major chondrogenic phenotypes in 4-week *ex vivo* IVD organ culture were almost identical to those in *in vivo* circumstance, indicating that *ex vivo* system could provide sufficient IVD tissues for evaluating reproducible and multiple independent experiment groups, minimizing the model of living animals [33,35].

Whole IVD organ culture systems have been developed to preserve healthy tissue architecture and cellular physiology in IVD regeneration studies [12,13,32,35]. However, diseased IVD with pathological characterizations such as degraded disc matrix and degenerative NP cells were not presented in healthy IVD organ cultures. Thus, chemonucleolytic agents including trypsin, chymopapain and chondroitinase ABC, etc. that specifically digest GAG chains in disc matrix have been widely applied in animal model to mimic disc degeneration [31,36,37]. Once the matrix is degraded, in which the disc cells will then go through apoptosis. Therefore, the optimal dose of chemonucleolytic agent to create a partial digestion for keeping the residual NP cells as template mimicking the degeneration is critical in the model. Different doses of chymopapain were applied to create degenerative disc model (Fig. 1C). While 200 U chymopapain was injected into the central of disc for 1 week, significant defect space was shown in NP tissue. Besides, the remaining NP cells with intensive GAG signals surrounding the cavity can be further used as a template for NP regeneration by therapeutic substrates. Taken together, our results showed that chymopapain-induced disc defects in *ex vivo* were supported by those in *in vivo* (Fig. 3, I-D and II-B, right panel).

Chondrogenic tissue engineering with mesenchymal stem cells (MSC) has been demonstrated in our previous studies [21,22]. To determine whether MSC could restore the chymopapain-induced disc degeneration, an MSC cell line cloned from the bone marrow of GFP-transgenic porcine (MSC-GFP) was applied. The multilineage potentials of MSC-GFP were characterized under specialized conditions without affecting their intensity of GFP expression (Fig. 2), which can be monitored in living cells and animals for tissue engineering in this study and others [38,39]. In addition, improvement of imaging strategies would promote stem-cell-driven tissue regeneration to be fully illustrated in mammals [40]. Fig. 3I-A showed that the implanted MSC-GFP could be monitored for cell proliferation in 4-week *ex vivo* culture disc by optical imaging system (IVIS 200, Xenogen Corporation), which was confirmed by immunohistochemistry (IHC) with anti-GFP antibody (Fig. 3, I-D) and supported by the 2-month *in vivo* implantation (Fig. 3, II-B). Due to the avascular environment of NP tissue and nonimmunogenic or hypoimmunogenic phenotypes of MSC, implanted MSC can proliferate in *in vivo* disc circumstance without attacked by immune system of hosts [19,41]. Hence, the massive *ex vivo* organ culture might be considered as an easier approach for translational research in IVD regeneration.

After 4-week *ex vivo* culture, the implanted MSC-GFP group showed increasing chondrogenic phenotypes of NP including Col II and aggrecan in newly regenerative tissue (Fig. 3, I-B), indicating the differentiation of MSC-GFP to NP cells. The potentials of MSC differentiation into NP-like cells have been reported in *in vitro* and *in vivo* models [15,19,42,43]. Richardson et al. also demonstrated IVD cell-mediated MSC differentiation and the potential of stem cell based IVD regeneration [20]. However, the differentiation mechanisms of MSC by chondrocytes were still unclear. Microenvironment niche plays an important role in regulating the proliferation and differentiation of stem cells [44]. Previously, we have demonstrated the adult chondrocytes committing stem cells into chondroprogenitors through a stage-specific molecular pathways [21]. The pathway, including cell–cell interaction, mesenchymal condensation, differentiation and terminal differentiation, was characterized and similar to the developmental process of mesenchyme *in vivo*. We also found that transforming growth factor-β1 (TGF-β1), fibroblast growth factor-2 (FGF-2) and epithelial growth factor (EGF) genes were significantly and strongly upregulated during *in vitro* stage-specific chondrogenesis of stem cells committed by chondrocytes. In this study, these significant molecules were also confirmed in *ex vivo* IVD tissue culture which provides a naïve cell–matrix interaction to elucidate the chondrogenesis behavior of MSC-GFP commitment.

For growth factors therapy in IVD regeneration, many studies showed that PRP provided a natural growth factor resource to induce proteoglycan accumulation and tissue regeneration in disc [17,29,45,46]. We have previously demonstrated PRP promoting redifferentiation of NP cells through TGF-β1 pathway on human cell *in vitro* model [29]. Since the Smad2/3, a specific TGF-β1-induced signaling molecule, was phosphorylated and activated in chondrocytes, a series of redifferentiation processes were then proceeding. In addition, the major ingredient TGF-β1 was used as an indicator for PRP to be quantified. With PRP (TGF-β1 = 1 ng/ml) treatment, porcine NP cells showed a high proliferation and chondrogenic redifferentiation (Supplemental Fig. 1, A and C), which was supported by the human NP results in our previous study [29]. Furthermore, growth factors in PRP comprising insulin-like growth factor (IGF-I), epidermal growth factors (EGF) and platelet-derived growth factor (PDGF) have also been reported to stimulate cell proliferation, chondrogenic-specific gene upregulations and chondrogenic matrices accumulations of NP cells [26,47,48]. For therapeutic efficacy, PRP purified from porcine was also injected in both *ex vivo* and *in vivo* animal model and showed a large quantity of chondrogenic matrix accumulations in PRP injected region (Fig. 4, I-C and II-B).

Depletion of proteoglycan and collagen directly diminishes the hydrostastic pressure in IVD and causes disc collapse as well as disc height reduction [49]. In many chemonucleolytic agents, only chymopapain had been examined in human as a chemical dissolution of herniated NP and can specifically depolymerize the GAG components of disc proteoglycan [50]. In our *in vivo* results, obvious IVD collapse was also observed from X-ray images (data not shown). Disc height index (DHI), an important disc functional indicator, was reduced to 73 ± 16.96% after chymopapain (200 U) injection compared to normal control (Fig. 5B). However, DHI was significantly restored by a single *in vivo* injection of MSC-GFP and PRP after 2 months, respectively. Supported by the IHC results in *in vivo* therapeutic groups (Fig. 3, II-B; Fig. 4, II-B), proteoglycan matrices were abundantly recovered, and the regenerated tissue finally resulted in the increase of DHI *in vivo*.

Both *ex vivo* and *in vivo* IVD regeneration results showed that either MSC-GFP or PRP could induce chondrogenesis. Put together, MSC-GFP/PRP combined treatment will draw our interesting in either additive or synergistic efficacy. Before the combination therapy, we have examined the *in vitro* interaction of MSC-GFP with PRP. MSC-GFP cell viability was upregulated by PRP, however, osteogenesis but not chondrogenesis was detected during 7-day culture with PRP (Supplemental Fig. 1B and D). Similar to the *in vitro* results, co-injection of MSC-GFP with PRP in *ex vivo* organ culture showed an obvious cell proliferation from intensive fluorescent signals (Fig. 6A), and significantly osteogenic matrix accumulations from specific matrix staining after 4 weeks. Osteogenic or chondrogenic induction by PRP in tissue regeneration depends on their target cells and lineages. Other studies demonstrated that PRP enhanced MSC proliferation, osteogenesis, and *in vivo* bone

formation due to the undifferentiation property of MSC [51,52]. However, for well differentiated cells such as NP cells, PRP stimulated the chondrogenic redifferentiation and reconstitution of cartilaginous tissue [29,53]. Thus, our *in vitro* and *ex vivo* results indicated that the combination of MSC-GFP and PRP represented an unexpected and adverse therapeutic result for IVD regeneration instead of additive or synergistic manner.

To address strategies for disc regeneration, we focused on from earlier to intermediate degeneration stages. Based on clinical pathophysiology, severe disc degeneration resulted from compressive loading, shear stress and vibration, as well as aging, genetic, systemic and toxic factors would cause the irreversible disc structure deformation and diminish the normal disc function [54]. In addition, disc cells in severe disc degeneration may suffer imbalanced metabolic function and undergo cell apoptosis [19], thus, fail to respond to exogenous therapeutic substrates. In our experimental design, chymopapain-induced partial defect in *ex vivo* disc organ mimicking initial stage of *in vivo* disc degeneration with following advantages: (1) surrounding tissue including AF, transition zone (TZ), and endplate (EP) preserving healthy organization without enzymatic injured; (2) a portion of NP cells escaped from chymopapain digestion were preserved as template for tissue regeneration under biological treatment. Consequently, this platform is useful and could be considered as for preclinical drug screening.

5. Conclusions

In summary, the *ex vivo* tissue culture system successfully provided a new insight on tissue regeneration for human IVD. Its feasibilities have been demonstrated by both respective MSC- and PRP-based treatments that could also be manifested in *in vivo* animal model. As a result, we conclude that such an *ex vivo* degenerative IVD organ culture system has the potentials to substitute the complicated animal models and contribute to the drug discovery for clinical IVD regeneration.

Acknowledgements

This work is supported by the Core Facility grant (97-3112-B-010-016), National Science Council (Grant NSC, 97-2314-B-038-0330MY3), National Science Council (Grant NSC, 97-2627-E-002-002), HealthBanks Biotech Co., Ltd., Purzer pharmaceutical Co., Ltd and Kooper Biotech Co., Ltd.

Appendix

Figures with essential color discrimination. Most of the figures in this article have parts that are difficult to interpret in black and white. The full color images can be found in the online version, at doi:10.1016/j.biomaterials.2009.07.019.

Appendix. Supplementary data

Supplementary data associated with this article can be found in the online version, at doi:10.1016/j.biomaterials.2009.07.019.

References

[1] Takahashi K, Aoki Y, Ohtori S. Resolving discogenic pain. Eur Spine J 2008;17(Suppl. 4):428–31.
[2] Le Maitre CL, Pockert A, Buttle DJ, Freemont AJ, Hoyland JA. Matrix synthesis and degradation in human intervertebral disc degeneration. Biochem Soc Trans 2007;35(Pt 4):652–5.
[3] Inkinen RI, Lammi MJ, Lehmonen S, Puustjarvi K, Kaapa E, Tammi MI. Relative increase of biglycan and decorin and altered chondroitin sulfate epitopes in the degenerating human intervertebral disc. J Rheumatol 1998;25(3):506–14.
[4] Singh K, Masuda K, An HS. Animal models for human disc degeneration. Spine J 2005;5(6 Suppl.):267S–79S.
[5] An HS, Masuda K. Relevance of in vitro and in vivo models for intervertebral disc degeneration. J Bone Joint Surg Am 2006;88(Suppl. 2):88–94.
[6] Bradford DS, Cooper KM, Oegema Jr TR. Chymopapain, chemonucleolysis, and nucleus pulposus regeneration. J Bone Joint Surg Am 1983;65(9):1220–31.
[7] Bradford DS, Oegema Jr TR, Cooper KM, Wakano K, Chao EY. Chymopapain, chemonucleolysis, and nucleus pulposus regeneration. A biochemical and biomechanical study. Spine 1984;9(2):135–47.
[8] Kaapa E, Holm S, Han X, Takala T, Kovanen V, Vanharanta H. Collagens in the injured porcine intervertebral disc. J Orthop Res 1994;12(1):93–102.
[9] Lauerman WC, Platenberg RC, Cain JE, Deeney VF. Age-related disk degeneration: preliminary report of a naturally occurring baboon model. J Spinal Disord 1992;5(2):170–4.
[10] Drespe IH, Polzhofer GK, Turner AS, Grauer JN. Animal models for spinal fusion. Spine J 2005;5(6 Suppl.):209S–16S.
[11] Grunhagen T, Wilde G, Soukane DM, Shirazi-Adl SA, Urban JP. Nutrient supply and intervertebral disc metabolism. J Bone Joint Surg Am 2006;88(Suppl. 2):30–5.
[12] Haschtmann D, Stoyanov JV, Ettinger L, Nolte LP, Ferguson SJ. Establishment of a novel intervertebral disc/endplate culture model: analysis of an ex vivo in vitro whole-organ rabbit culture system. Spine 2006;31(25):2918–25.
[13] Zhang Y, Phillips FM, Thonar EJ, Oegema T, An HS, Roman-Blas JA, et al. Cell therapy using articular chondrocytes overexpressing BMP-7 or BMP-10 in a rabbit disc organ culture model. Spine 2008;33(8):831–8.
[14] Smith L. Enzyme dissolution of the nucleus pulposus in humans. JAMA 1964;187:137–40.
[15] Hiyama A, Mochida J, Iwashina T, Omi H, Watanabe T, Serigano K, et al. Transplantation of mesenchymal stem cells in a canine disc degeneration model. J Orthop Res 2008;26(5):589–600.
[16] Leung VY, Chan D, Cheung KM. Regeneration of intervertebral disc by mesenchymal stem cells: potentials, limitations, and future direction. Eur Spine J 2006;15(Suppl. 3):S406–13.
[17] Masuda K. Biological repair of the degenerated intervertebral disc by the injection of growth factors. Eur Spine J 2008;17(Suppl. 4):441–51.
[18] Risbud MV, Shapiro IM, Vaccaro AR, Albert TJ. Stem cell regeneration of the nucleus pulposus. Spine J 2004;4(6 Suppl.):348S–53S.
[19] Zhang YG, Guo X, Xu P, Kang LL, Li J. Bone mesenchymal stem cells transplanted into rabbit intervertebral discs can increase proteoglycans. Clin Orthop Relat Res 2005;430:219–26.
[20] Richardson SM, Walker RV, Parker S, Rhodes NP, Hunt JA, Freemont AJ, et al. Intervertebral disc cell-mediated mesenchymal stem cell differentiation. Stem Cells 2006;24(3):707–16.
[21] Chen WH, Lai MT, Wu AT, Wu CC, Gelovani JG, Lin CT, et al. In vitro stage-specific chondrogenesis of mesenchymal stem cells committed to chondrocytes. Arthritis Rheum 2009;60(2):450–9.
[22] Chen CW, Tsai YH, Deng WP, Shih SN, Fang CL, Burch JG, et al. Type I and II collagen regulation of chondrogenic differentiation by mesenchymal progenitor cells. J Orthop Res 2005;23(2):446–53.
[23] Ryan JM, Barry FP, Murphy JM, Mahon BP. Mesenchymal stem cells avoid allogeneic rejection. J Inflamm (Lond) 2005;2:8.
[24] Masuda K, Oegema Jr TR, An HS. Growth factors and treatment of intervertebral disc degeneration. Spine 2004;29(23):2757–69.
[25] Imai Y, Okuma M, An HS, Nakagawa K, Yamada M, Muehleman C, et al. Restoration of disc height loss by recombinant human osteogenic protein-1 injection into intervertebral discs undergoing degeneration induced by an intradiscal injection of chondroitinase ABC. Spine 2007;32(11):1197–205.
[26] Osada R, Ohshima H, Ishihara H, Yudoh K, Sakai K, Matsui H, et al. Autocrine/paracrine mechanism of insulin-like growth factor-1 secretion, and the effect of insulin-like growth factor-1 on proteoglycan synthesis in bovine intervertebral discs. J Orthop Res 1996;14(5):690–9.
[27] Tozum TF, Demiralp B. Platelet-rich plasma: a promising innovation in dentistry. J Can Dent Assoc 2003;69(10):664.
[28] Wadhwa M, Seghatchian MJ, Lubenko A, Contreras M, Dilger P, Bird C, et al. Cytokine levels in platelet concentrates: quantitation by bioassays and immunoassays. Br J Haematol 1996;93(1):225–34.
[29] Chen WH, Lo WC, Lee JJ, Su CH, Lin CT, Liu HY, et al. Tissue-engineered intervertebral disc and chondrogenesis using human nucleus pulposus regulated through TGF-beta1 in platelet-rich plasma. J Cell Physiol 2006;209(3):744–54.
[30] Rashid ST, Salacinski HJ, Hamilton G, Seifalian AM. The use of animal models in developing the discipline of cardiovascular tissue engineering: a review. Biomaterials 2004;25(9):1627–37.
[31] Roberts S, Menage J, Sivan S, Urban JP. Bovine explant model of degeneration of the intervertebral disc. BMC Musculoskelet Disord 2008;9:24.
[32] Risbud MV, Di Martino A, Guttapalli A, Seghatoleslami R, Denaro V, Vaccaro AR, et al. Toward an optimum system for intervertebral disc organ culture: TGF-beta 3 enhances nucleus pulposus and anulus fibrosus survival and function through modulation of TGF-beta-R expression and ERK signaling. Spine 2006;31(8):884–90.
[33] Alini M, Eisenstein SM, Ito K, Little C, Kettler AA, Masuda K, et al. Are animal models useful for studying human disc disorders/degeneration? Eur Spine J 2008;17(1):2–19.
[34] Kale S, Biermann S, Edwards C, Tarnowski C, Morris M, Long MW. Three-dimensional cellular development is essential for ex vivo formation of human bone. Nat Biotechnol 2000;18(9):954–8.

[35] Korecki CL, MacLean JJ, Iatridis JC. Characterization of an in vitro intervertebral disc organ culture system. Eur Spine J 2007;16(7):1029–37.
[36] Melrose J, Taylor TK, Ghosh P, Holbert C, Macpherson C, Bellenger CR. Intervertebral disc reconstitution after chemonucleolysis with chymopapain is dependent on dosage. Spine 1996;21(1):9–17.
[37] Norcross JP, Lester GE, Weinhold P, Dahners LE. An in vivo model of degenerative disc disease. J Orthop Res 2003;21(1):183–8.
[38] Misteli T, Spector DL. Applications of the green fluorescent protein in cell biology and biotechnology. Nat Biotechnol 1997;15(10):961–4.
[39] Hara M, Murakami T, Kobayashi E. In vivo bioimaging using photogenic rats: fate of injected bone marrow-derived mesenchymal stromal cells. J Autoimmun 2008;30(3):163–71.
[40] Schroeder T. Imaging stem-cell-driven regeneration in mammals. Nature 2008;453(7193):345–51.
[41] Majumdar MK, Keane-Moore M, Buyaner D, Hardy WB, Moorman MA, McIntosh KR, et al. Characterization and functionality of cell surface molecules on human mesenchymal stem cells. J Biomed Sci 2003;10(2):228–41.
[42] Risbud MV, Albert TJ, Guttapalli A, Vresilovic EJ, Hillibrand AS, Vaccaro AR, et al. Differentiation of mesenchymal stem cells towards a nucleus pulposus-like phenotype in vitro: implications for cell-based transplantation therapy. Spine 2004;29(23):2627–32.
[43] Vadala G, Studer RK, Sowa G, Spiezia F, Iucu C, Denaro V, et al. Coculture of bone marrow mesenchymal stem cells and nucleus pulposus cells modulate gene expression profile without cell fusion. Spine 2008;33(8):870–6.
[44] Moore KA, Lemischka IR. Stem cells and their niches. Science 2006;311(5769):1880–5.
[45] Akeda K, An HS, Pichika R, Attawia M, Thonar EJ, Lenz ME, et al. Platelet-rich plasma (PRP) stimulates the extracellular matrix metabolism of porcine nucleus pulposus and anulus fibrosus cells cultured in alginate beads. Spine 2006;31(9):959–66.
[46] Anitua E, Sanchez M, Orive G, Andia I. The potential impact of the preparation rich in growth factors (PRGF) in different medical fields. Biomaterials 2007;28(31):4551–60.
[47] Gruber HE, Norton HJ, Hanley Jr EN. Anti-apoptotic effects of IGF-1 and PDGF on human intervertebral disc cells in vitro. Spine 2000;25(17):2153–7.
[48] Konttinen YT, Kemppinen P, Li TF, Waris E, Pihlajamaki H, Sorsa T, et al. Transforming and epidermal growth factors in degenerated intervertebral discs. J Bone Joint Surg Br 1999;81(6):1058–63.
[49] Luoma K, Vehmas T, Riihimaki H, Raininko R. Disc height and signal intensity of the nucleus pulposus on magnetic resonance imaging as indicators of lumbar disc degeneration. Spine 2001;26(6):680–6.
[50] Gibson MJ, Buckley J, Mulholland RC, Worthington BS. The changes in the intervertebral disc after chemonucleolysis demonstrated by magnetic resonance imaging. J Bone Joint Surg Br 1986;68(5):719–23.
[51] Vogel JP, Szalay K, Geiger F, Kramer M, Richter W, Kasten P. Platelet-rich plasma improves expansion of human mesenchymal stem cells and retains differentiation capacity and in vivo bone formation in calcium phosphate ceramics. Platelets 2006;17(7):462–9.
[52] Arpornmaeklong P, Kochel M, Depprich R, Kubler NR, Wurzler KK. Influence of platelet-rich plasma (PRP) on osteogenic differentiation of rat bone marrow stromal cells. An in vitro study. Int J Oral Maxillofac Surg 2004;33(1):60–70.
[53] Wu W, Chen F, Liu Y, Ma Q, Mao T. Autologous injectable tissue-engineered cartilage by using platelet-rich plasma: experimental study in a rabbit model. J Oral Maxillofac Surg 2007;65(10):1951–7.
[54] Hadjipavlou AG, Tzermiadianos MN, Bogduk N, Zindrick MR. The pathophysiology of disc degeneration: a critical review. J Bone Joint Surg Br 2008;90(10):1261–70.